applied sciences

MDPI

Article

Transportation of Objects on an Inclined Plane Oscillating in the Longitudinal Direction Applying Dynamic Dry Friction Manipulations

Ribal El Banna [1,*], Kristina Liutkauskienė [2], Vaidas Lukoševičius [1], Algimantas Fedaravičius [1] and Sigitas Kilikevičius [1]

[1] Department of Transport Engineering, Kaunas University of Technology, Studentų St. 56, 51424 Kaunas, Lithuania; vaidas.lukosevicius@ktu.lt (V.L.); algimantas.fedaravicius@ktu.lt (A.F.); sigitas.kilikevicius@ktu.lt (S.K.)

[2] Department of Mechanical Engineering, Kaunas University of Technology, Studentų St. 56, 51424 Kaunas, Lithuania; kristina.liutkauskiene@ktu.lt

* Correspondence: ribal.el@ktu.edu

Abstract: A transportation system requires an asymmetry to achieve objects' motion on an oscillating surface. Transportation methods based on vibrational techniques usually employ different types of asymmetries, such as temporal (time) asymmetry, kinematic asymmetry, wave asymmetry or power asymmetry. However, transporting an object on an inclined angle requires a relatively high net frictional force over each period of vibrational cycles due to the gravitational potential energy exerted on the object. This paper investigates the transportation of an object upward on an inclined plane that harmonically oscillates in its longitudinal direction. The novelty of this research is attributed to the upward motion of the object on the inclined plane, which is achieved by creating an additional asymmetry of the system through dry friction dynamic manipulations. For this reason, periodic dynamic dry friction manipulations have been employed to create the asymmetry of frictional conditions, resulting in a net frictional force that outweighs the gravitational force. A mathematical model has been developed using the Lagrange method, which describes the moving object's motion. Moreover, the theoretical findings and results confirmed that the object's velocity and direction can be controlled by dynamic dry friction manipulations. To demonstrate the technical feasibility of the proposed method, an experimental investigation was carried out where the results demonstrated that the control parameters significantly influence the characteristics of the directional motion of the moving object. This transportation method is beneficial for various modern industries engaged in transportation and manipulation tasks with objects spanning a broad range of sizes, including those operating at small scales for applications in lab-on-a-chip technology, micro-assembly lines, micro-feeder systems and other delicate component manipulation systems. The presented research advances the classical theories of vibrational transportation on inclined surfaces.

Keywords: vibrational transport; asymmetry; inclined plane; harmonically oscillating plane; dynamic dry friction manipulations

Citation: El Banna, R.; Liutkauskienė, K.; Lukoševičius, V.; Fedaravičius, A.; Kilikevičius, S. Transportation of Objects on an Inclined Plane Oscillating in the Longitudinal Direction Applying Dynamic Dry Friction Manipulations. *Appl. Sci.* **2024**, *14*, 4474. https://doi.org/10.3390/app14114474

Academic Editor: Muhammad Junaid Munir

Received: 2 April 2024
Revised: 15 May 2024
Accepted: 21 May 2024
Published: 24 May 2024

1. Introduction

Transport and manipulation of various objects can be implemented using various methods and approaches. The usage of vibrational transport has significantly increased in several disciplines and sectors, such as micro-machine technology, biotechnology, cell biology, material processing, semiconductors and neuroscience [1–3].

To perform vibrational transport tasks effectively, asymmetry is an essential condition to achieve the motion of a part on a plane. In the presence of asymmetry, the net friction force throughout a single oscillation is not nullified, which drives the motion of transported objects. Transportation methods that rely on vibrational techniques commonly utilize temporal asymmetry, spatial asymmetry, power (force) asymmetry, kinematic asymmetry, or wave asymmetry to achieve the part's motion.

Temporal asymmetry, also known as time asymmetry, can be achieved through different forward and backward speeds, where the forward motion takes longer than the backward motion. Reznik et al. [4] studied the transportation of objects placed on a vibrating pane exposed to vibrational excitation where the velocity of the forward motion was not equal to the velocity of the backward motion in each vibration cycle. This sort of vibrational excitation resulted in a temporal asymmetry necessary to perform the transportation task. Viswarupachari et al. [5] studied the transportation of particles on a rigid plane subjected to asymmetrical vibrations that resulted in a temporal asymmetry. Mayyas [6,7] investigated the stick–slip dynamics of a part transporting on a two-dimensional oscillating plane, where a temporal asymmetry is employed to achieve the motion of an object. In this case, the object moved forward when the platform acceleration in the forward direction created an inertial force lower than the friction force. Hunnekens et al. [8] demonstrated that a proper periodic motion profile of a vibrating plane results in a temporal asymmetry that can be used to transport an object.

According to the theory of vibrational transportation, if the transportation system is inclined with respect to the horizontal plane or a constant force is applied to the object to be transported, then a power asymmetry is induced. Higashimori et al. [9] proposed a method that uses vibrations on a plate, where a power asymmetry is accomplished by changing the frequency and the offset angle of the vibrational platform connected to an actuator. The direction of the part in motion is controlled and reached by exploiting asymmetric platform oscillations achieved due to different frequencies with a phase shift for the x and y axis. Sakashita et al. [10] and Yamaguchi et al. [11] presented an experimental study implemented using an excitation vibrating plate, where a single actuator is used to control the motion of a part in 3-DoF (degree of freedom). The results revealed that the translation and rotation of a part could be governed by tuning the offset angle and sinusoidal excitation of the actuator through the asymmetric vibrational orbit of the platform. Chen et al. [12] analyzed the particle conveyance mechanism using a discrete element method (DEM). In this case, an asymmetric force was achieved, which led to particle directional conveyance, where the velocity increases with the increase in vibration time.

Asymmetries of the vibration path or the law of motion along this path are classified as kinematic asymmetries. Vrublevskyi [13] investigated vibrational transportation achieved through a kinematic asymmetry where an inclined platform was subjected to harmonic longwise and polyharmonic perpendicular oscillations. This type of asymmetry is usually applied to various industrial vibrational transportation applications [14–16]. Baksys and Baskutiene [17] investigated the characteristics of the motion of the compliant body subjected to kinematic excitations along the direction of the joining axis. Moreover, Baksys and Puodziuniene [18] have investigated the body motion from a static state to dynamic equilibrium by using vibrational non-impact displacement of an exited-based body on an inclined plane, where different asymmetries such as power asymmetry and kinematical asymmetry are combined.

Wave asymmetry occurs when the object moves in the same direction as the propagation of the traveling wave [19]. Kumar and Dasgupta [20] analyzed the circumferential traveling wave on a thin circular plate. Three circumferentially actuators are connected to the circular plate and positioned at the excited plate transversely to a relevant phasing, where wave asymmetry is achieved.

Recently, a novel approach for omnidirectional vibrational transportation has been proposed [21,22]. The omnidirectional motion of an object on a horizontal platform subjected to harmonic circular motion was achieved and controlled through an asymmetry induced by periodic dynamic dry friction control between the object and the platform.

This research aims to uncover the feasibility of transporting objects upward on an inclined plane that harmonically oscillates in its longitudinal direction by applying an additional asymmetry achieved through dynamic dry friction manipulations, as well as to determine the control parameters of the transportation process.

2. Methodology

2.1. Mathematical Model Using Lagrangian Mechanics

Figure 1 depicts the dynamic model of the transportation of objects on an inclined plane harmonically oscillating in its longitudinal direction.

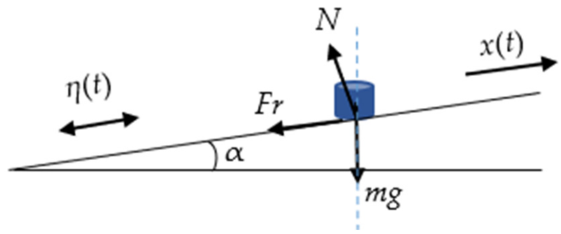

Figure 1. Dynamic model of transportation of objects on an inclined plane oscillating in its longitudinal direction.

The inclined plane is subjected to harmonic oscillations along its longitudinal direction:

$$\eta(t) = A\sin(\omega t), \tag{1}$$

where η is the displacement of the platform, A is the amplitude, ω is the angular frequency of the harmonic excitation along the longitudinal direction, and t is the time.

The Lagrange equation represents the difference between kinetic and potential energy, as shown in Equation (2).

$$L = T + F_r\dot{x} - U, \tag{2}$$

where T corresponds to the translational kinetic energy of the object being transported, m is the object's mass, F_r is the dry friction force between the object and the inclined plane, x is the displacement of the object along the inclined plane, and U is the potential energy.

$$T = \frac{1}{2}\,m\left(\dot{x} + \dot{\eta}\right)^2 = \frac{1}{2}m\dot{x}^2 + mA\omega\cos(\omega t)\dot{x} + \frac{1}{2}mA^2\omega^2\cos^2(\omega t), \tag{3}$$

$$U = mgx\sin\alpha, \tag{4}$$

$$F_r\dot{x} = \mu(\omega t)mg\cos(\alpha)\left(\dot{x} + \dot{\eta}\right)\mathrm{sign}(\dot{x}), \tag{5}$$

where g is the gravity, α is the inclination angle of the oscillating platform, and $\mu(\omega t)$ is the effective dry friction coefficient, where, in this study, it is considered as a periodic function of the same period as the longitudinal harmonic oscillations of the platform.

The Euler–Lagrange equation was written as shown in Equation (6).

$$\frac{d}{dt}\frac{\partial L}{\partial \dot{x}} - \frac{\partial L}{\partial x} + \frac{\partial\left(F_r\dot{x}\right)}{\partial \dot{x}} = 0. \tag{6}$$

Equation (7) shows the partial derivative of the Lagrange equation that describes the momentum of the moving particle on an inclined plane.

$$\frac{d}{dt}\frac{\partial L}{\partial \dot{x}} = m\ddot{x} - mA\omega^2\sin(\omega t). \tag{7}$$

The rate of change of momentum can be affected and changed due to the potential energy and the friction forces exerted on the moving object on an inclined plane, as shown in Equations (8) and (9), respectively.

$$\frac{\partial L}{\partial x} = -mg\sin(\alpha), \tag{8}$$

$$\frac{\partial(F_r\dot{x})}{\partial\dot{x}} = \mu(\omega t)mg\cos(\alpha)\text{sign}(\dot{x}),$$
$$\text{where}\begin{cases} F_r = mg\cos(\alpha)\mu(\omega t)\text{sign}(\dot{x}), \dot{x} \neq 0 \\ -mg\cos(\alpha)\mu(\omega t) < F_r < mg\cos(\alpha)\mu(\omega t),\ \dot{x} = 0 \end{cases} \tag{9}$$

Non-dimensionalization was applied to identify and determine the characteristic control parameters:

$$\tau = \omega t,\ \xi = x/A,\ \ \gamma = g/A\omega^2, \tag{10}$$

The following non-dimensional equation can describe the relative body motion on the inclined plane:

$$\xi'' = \sin(\tau) - \gamma(\sin(\alpha) + \mu(\tau)\cos(\alpha)\text{sign}(\xi')), \tag{11}$$

The average non-dimensional velocity of the moving object is presented in Equation (12):

$$\langle\xi'\rangle = \frac{1}{2\pi}\int_0^{2\pi}\xi' d\tau, \tag{12}$$

To achieve the additional asymmetry needed for the upward motion of the object, the dry friction coefficient magnitude is periodically manipulated in each cycle of oscillations of the inclined plane. With respect to the period harmonic excitations, the dry friction is being manipulated by a rectangular function, as shown in Figure 2.

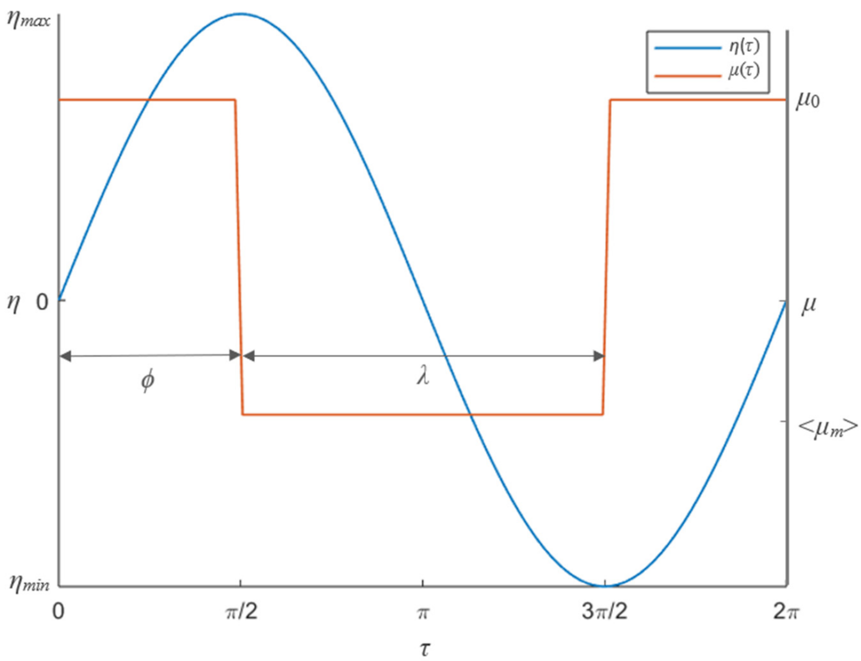

Figure 2. Schematic presentation of dynamic friction manipulations with respect to the period of harmonic oscillations.

The rectangular function that represents the dynamic dry friction manipulations with respect to the longitudinal harmonic oscillations can be described by the following equation:

$$\mu(\tau) = \begin{cases} \langle\mu_m\rangle, \text{ when } \phi + 2\pi n < \tau < \phi + \lambda + 2\pi n \\ \mu_0, \text{ otherwise} \end{cases} \tag{13}$$

where n represents the number of cycles of the harmonic oscillations of the inclined plane n = (0, 1, 2, 3. . .N), μ_0 is the nominal dry friction coefficient between the object and the platform's surface. $\langle \mu_m \rangle$ is the dry friction coefficient between the object and the platform's surface that is dynamically modified, λ corresponds to the part of the period in which the friction coefficient is dynamically decreased to an effective value of $\langle \mu_m \rangle$ as presented in Figure 2. The ratio $\langle \mu_m \rangle / \mu_0$ indicates the extent to which the dynamic modification of the dry friction coefficient deviates from the nominal dry friction coefficient. This parameter can be associated with the magnitude of the frictional asymmetry. ϕ is the phase shift between the function of harmonic oscillations and the function governing the dry friction coefficient. Therefore, these dynamic friction manipulations generate an asymmetry of frictional conditions to move the object on an inclined platform upward.

In terms of practicality, the dry friction coefficient can be manipulated dynamically by means of high-frequency vibrations generated between contacting objects. Research reported in numerous papers demonstrates a reduction in frictional forces between sliding bodies in the presence of vibrations [23–27].

2.2. Experimental Investigation

An experimental study has been carried out to verify the proposed method's feasibility. The concept behind this experiment was to transport a small-scaled object on a harmonically oscillating inclined plane upwards through dynamic dry friction manipulations.

The principle diagram shown in Figure 3a represents the experimental setup for transporting an object on an inclined plane oscillating in the longitudinal direction implemented through dynamic dry friction manipulation. Figure 3b shows the general view of the experimental setup. The experimental setup consists of an inclined plane (1) and the transportation surface (2) that was mounted on top of a piezoelectric actuator (3) that was used for dry friction dynamic manipulations through bursts of high-frequency vibrations. The moving object was placed on the transportation surface. The roughness of the manipulated surface was around 0.2 µm. The inclined plane was subjected to low-frequency harmonic oscillations in the longitudinal direction created by an electrodynamic vibrator (ESE 211, VEB Robotron-Meßelektronik, Dresden, Germany) (4). A vibration sensor (5) monitored and controlled the harmonic oscillations. A power amplifier (LV-103, Metra Mess- und Frequenztechnik in Radebeul, Radebeul, Germany) (6) was used to amplify the harmonic signals to drive the electrodynamic vibrator. A piezo linear amplifier (EPA-104, Piezo Systems Inc., Cambridge, MA, USA) (7) was used to amplify the signals subjected to the piezoelectric actuator. A waveform generator (DG4202, RIGOL, Beijing, China) (8) was used to generate the signals. The signals were visualized and monitored using a digital oscilloscope (DS1054, RIGOL, Beijing, China) (9). The transportation of the object ($\phi 6 \times 0.7$ mm, 0.201 g) was captured and filmed using a camera connected to a PC (10,11). Then, the videos were divided into frames (40 frames/sec) and the moving object's trajectory was analyzed using MATLAB R2023a software.

The dry friction between the object and the transportation surface was dynamically manipulated by bursts of high-frequency vibrations (5860 Hz) that were periodically excited in a direction perpendicular to the manipulation plane by the piezoelectric actuator (Figure 3a). This frequency was close to the resonance frequency of the system, resulting in the most efficient reduction in the frictional properties. The bursts excited by the piezoelectric actuator were synchronized with respect to the period of the longitudinal oscillations, as shown in Figure 2. Therefore, the λ parameter was controlled by changing the amount of high-frequency waves in a burst and the parameter ϕ was changed by changing the phase shift between the harmonic signal and the signal for the piezoelectric actuator. Figure 4 shows an oscillogram to demonstrate the synchronized signals of piezoelectric actuator excitation and harmonic oscillation.

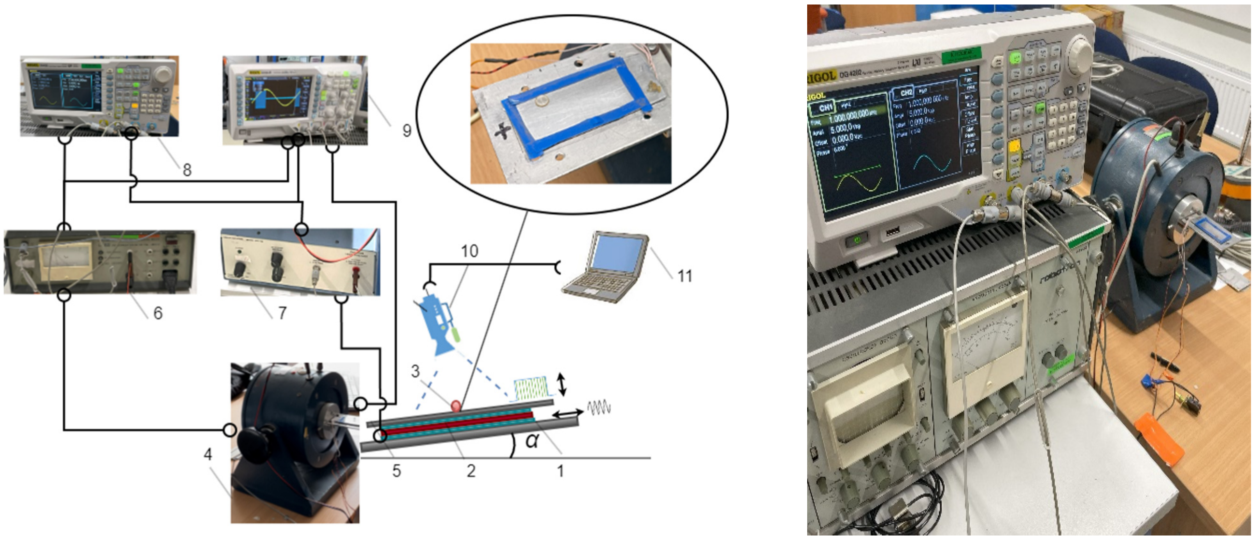

(**a**) (**b**)

Figure 3. Experimental setup for transportation of an object on an inclined plane by employing dynamic dry friction manipulations. (**a**) Principle diagram: (1) inclined plane; (2) piezoelectric actuator; (3) transportation surface; (4) electrodynamic vibrator; (5) vibration sensor; (6) power amplifier; (7) piezo linear amplifier; (8) waveform generator; (9) digital oscilloscope; (10) camera; (11) PC. (**b**) General view of the experimental setup.

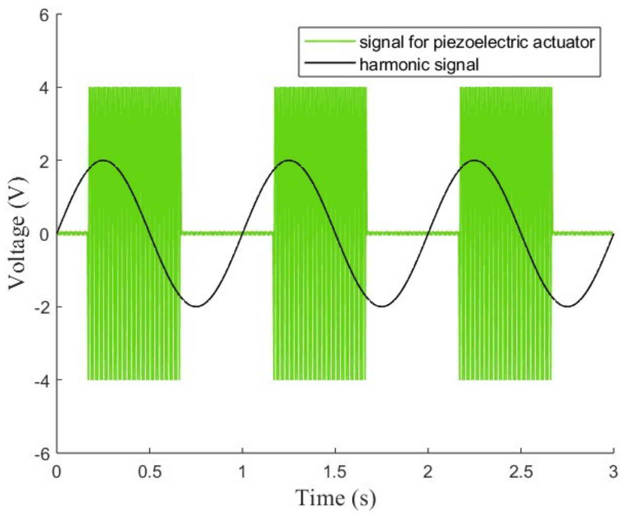

Figure 4. Oscillogram of the piezoelectric actuator and harmonic oscillations signals ($\phi = \pi/3$, $\lambda = \pi$ and $\omega = 62.83$ rad/s).

3. Results

3.1. Modeling Results

The mathematical model that describes the motion of an object on an inclined plane has been solved numerically using MATLAB R2023a software. The Runge–Kutta ordinary differential equation solver ode45 was used to solve the non-dimensional differential equation.

Figure 5 represents the non-dimensional average velocity depending on the phase shift ϕ at various inclination angles. The results have shown that the directional motion of the moving particle can be controlled by changing the phase shift ϕ. The average velocity was significantly increased at $\alpha = 0.035$ rad between $\phi = 0$ and $\phi = \pi/2$ and reached its maximum at $\lambda = \pi$, and then the average velocity was gradually decreased between $\phi = \pi/2$ and $\phi = 3\pi/2$, as shown in Figure 5a. However, as the inclination angle was increased to $\alpha = 0.1$ rad, the non-dimensional average velocity was significantly decreased between

$\phi = \pi/2$ and $\phi = \pi$ due to the potential energy that is exerted on the moving particle, as demonstrated in Figure 5b, where $\mu_0 = 0.2$ and $\langle\mu_m\rangle/\mu_0 = 1/5$. Therefore, ϕ is an essential parameter to control the direction of the moving object.

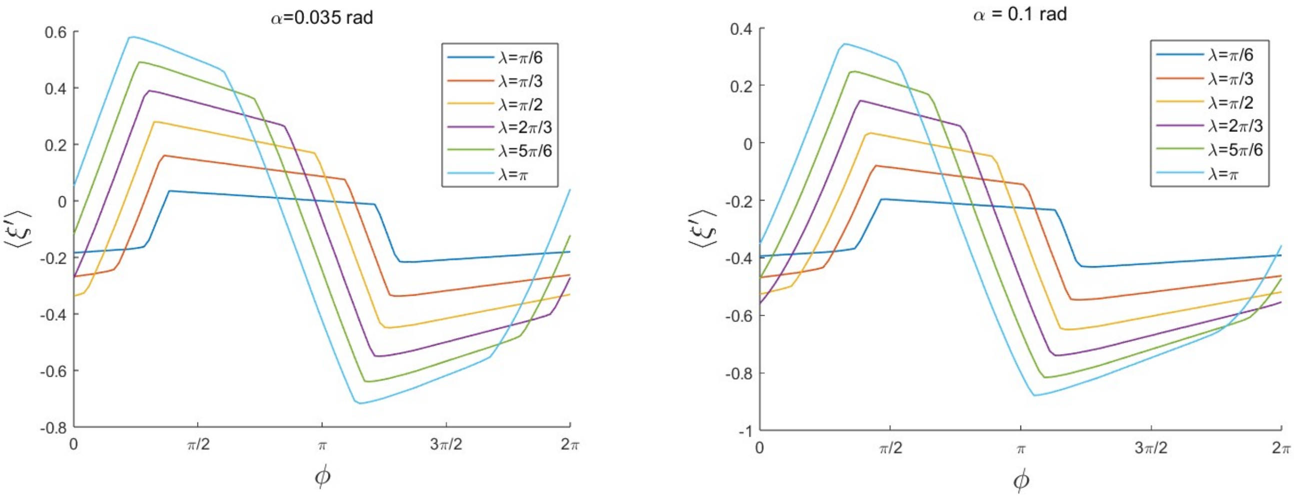

(**a**) (**b**)

Figure 5. Non-dimensional average velocity vs. the phase shift ϕ: (**a**) $\alpha = 0.035$ rad, $\gamma = 1$, $\mu_0 = 0.2$, $\langle\mu_m\rangle/\mu_0 = 1/5$; (**b**) $\alpha = 0.1$ rad, $\gamma = 1$, $\mu_0 = 0.2$, $\langle\mu_m\rangle/\mu_0 = 1/5$.

Since λ is a parameter that corresponds to the level of the frictional asymmetry, at $\alpha = 0.035$ rad, which is almost equivalent to 2 degrees of inclination angle, the average velocity was gradually increased and reached a maximum between $\lambda = \pi$ and $\lambda = 2\pi/3$ at $\phi = \pi/4$. Then, the average velocity was sharply decreased, and the particle moved downward in the opposite direction at $\lambda = 2\pi$, as shown in Figure 6a. The average velocity was slightly increased at $\alpha = 0.1$ rad and reached a maximum between $\lambda = \pi$ and $\lambda = 3\pi/2$, then it drastically decreased at $\lambda = 2\pi$ and then, the object started to move backward in a negative direction, as presented in Figure 6b. Therefore, λ is a crucial parameter to control the velocity of the moving particle on an inclined plane.

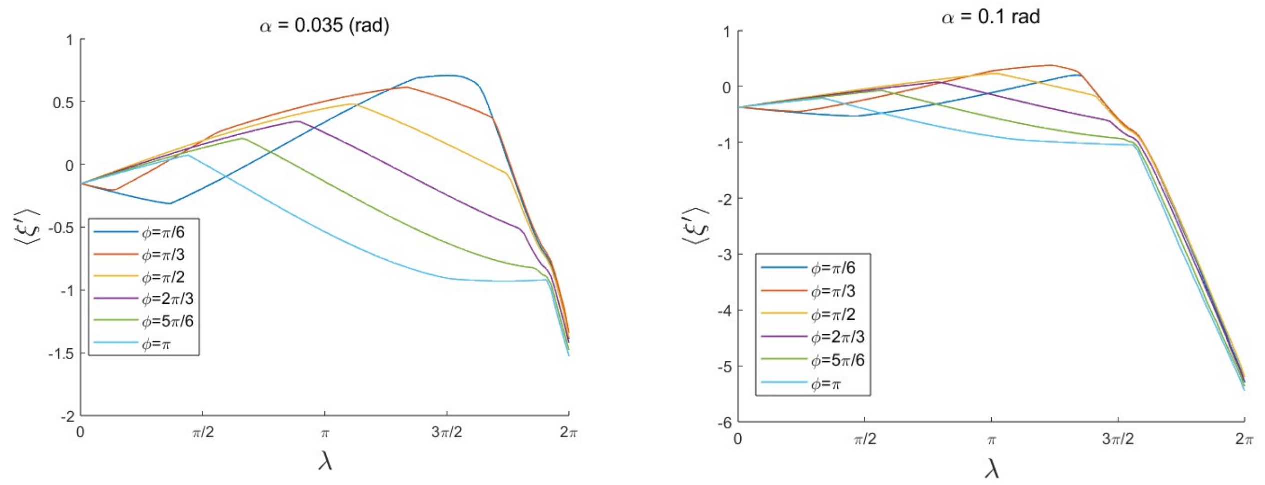

(**a**) (**b**)

Figure 6. Non-dimensional average velocity vs. λ: (**a**) $\alpha = 0.035$ rad, $\gamma = 1$, $\mu_0 = 0.2$, $\langle\mu_m\rangle/\mu_0 = 1/5$; (**b**) $\alpha = 0.1$ rad, $\gamma = 1$, $\mu_0 = 0.2$, $\langle\mu_m\rangle/\mu_0 = 1/5$.

The modeling has demonstrated that the ratio of the modified effective dry friction coefficient $\langle \mu_m \rangle$ to the nominal dry friction coefficient μ_0 has yielded a notable influence on the non-dimensional average velocity of moving objects. The average velocity was significantly decreased as $\langle \mu_m \rangle / \mu_0$ increased at $\alpha = 0.035$ rad. However, the average velocity of the moving object reached a maximum at $\mu_0 = 0.15$ and a minimum at $\mu_0 = 0.55$, as presented in Figure 7a. Nevertheless, the average velocity gradually decreased when the inclination angle increased to $\alpha = 0.1$ rad. The average velocity was dramatically reduced when this ratio increased from $\langle \mu_m \rangle / \mu_0 = 0.1$ to $\langle \mu_m \rangle / \mu_0 = 0.5$, as shown in Figure 7b.

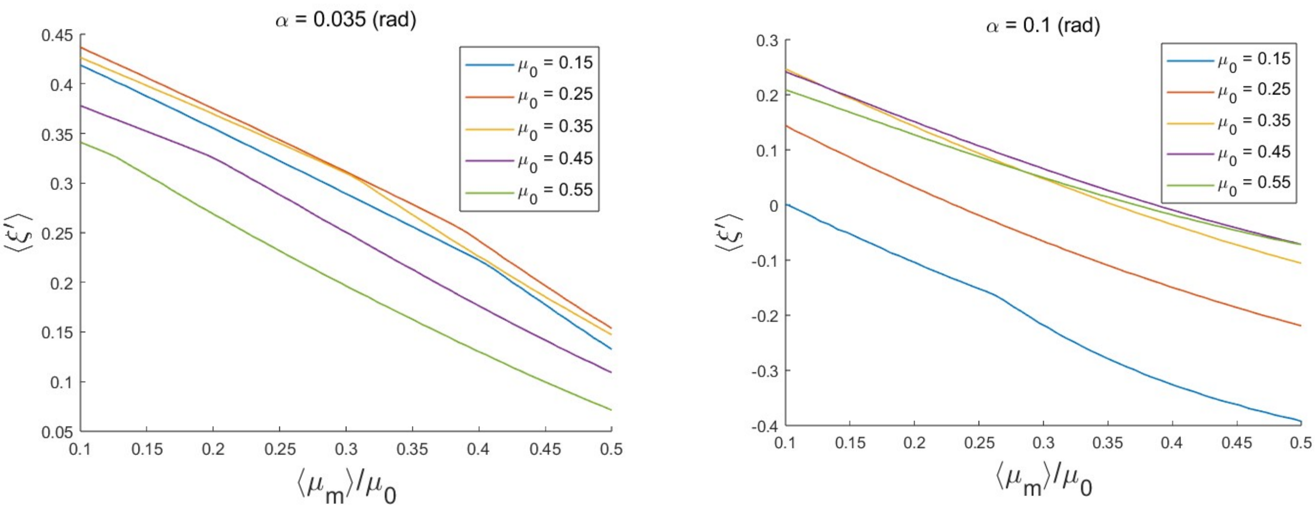

(**a**) (**b**)

Figure 7. Non-dimensional average velocity vs. the dry friction coefficient manipulation ratio: (**a**) $\alpha = 0.035$ rad, $\gamma = 1$, $\lambda = \pi$, $\phi = \pi/2$; (**b**) $\alpha = 0.1$ rad, $\gamma = 1$, $\lambda = \pi$, $\phi = \pi/2$.

The results have revealed that the directional motion of the object is also affected by γ ratio, which represents the gravity divided by amplitude multiplied by squared angular frequency as shown in Equation (10). The average velocity was gradually decreased between $\gamma = 1$ and $\gamma = 6$. The highest values were observed at $\lambda = 2\pi/3$, $\phi = \pi/2$, as demonstrated in Figure 8a. As the inclination angle was increased to 0.035 rad, the average velocity of an object was slightly increased and reached its highest values between $\gamma = 1$ and $\gamma = 4$, and then it started to decrease due to the gravitational potential energy exerted on it as shown in Figure 8b, where the ratio of the modified effective dry friction coefficient $\langle \mu_m \rangle / \mu_0$ is 1/5 and $\mu_0 = 0.2$.

The phase shift ϕ and another crucial parameter λ have significantly influenced the average velocity because they manipulate the shift and level of the frictional asymmetry. The object's average velocity dramatically decreased between $\alpha = 0$ rad and $\alpha = 0.12$ rad. This is due to the impact of the gravitation force exerted on it, where the non-dimensional average velocity reached the maximum at $\lambda = \pi$, $\phi = \pi/3$ and minimum at $\lambda = 2\pi/3$, $\phi = \pi/2$, as shown in Figure 9a. Moreover, the interpretation of the effect of the inclination angle on gamma is shown in Figure 9b. At a lower value of gamma, the average velocity has reached the maximum because the angular frequency at $\gamma = 1$ is higher than the angular frequency at $\gamma = 6$, where the average velocity steadily decreased between $\alpha = 0$ rad and $\alpha = 0.1$ rad at $\mu_0 = 0.2$, $\langle \mu_m \rangle / \mu_0 = 1/5$, $\lambda = \pi$ and $\phi = \pi/4$.

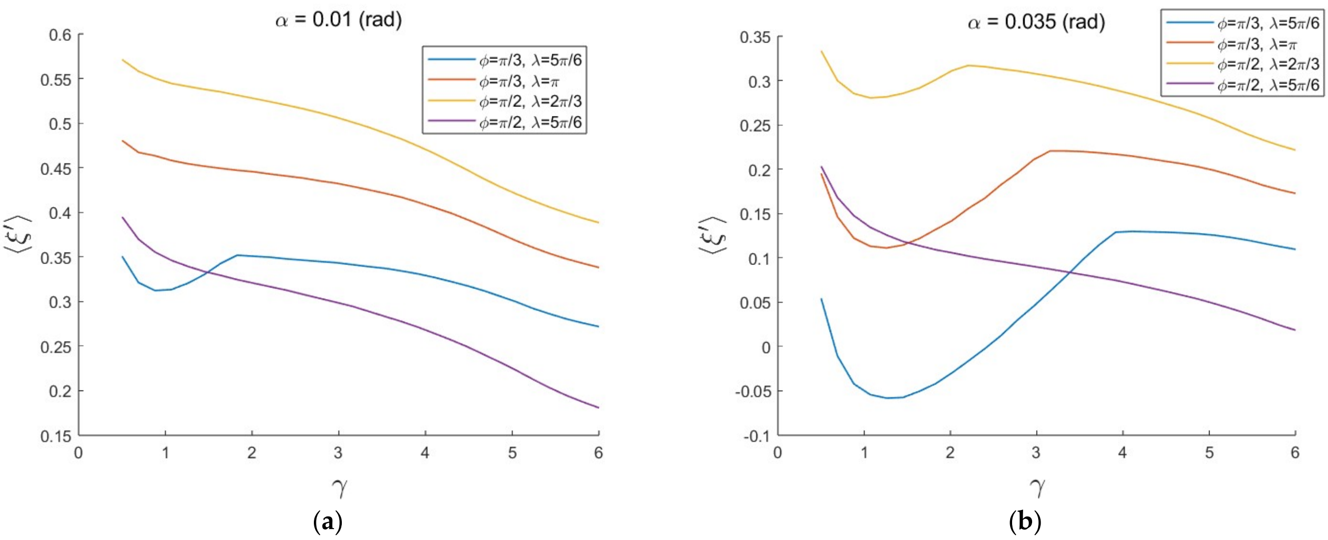

Figure 8. Non-dimensional average velocity vs. γ: (**a**) α = 0.01 rad, μ_0 = 0.2, $\langle\mu_m\rangle/\mu_0$ = 1/5; (**b**) α = 0.035 rad, μ_0 = 0.2, $\langle\mu_m\rangle/\mu_0$ = 1/5.

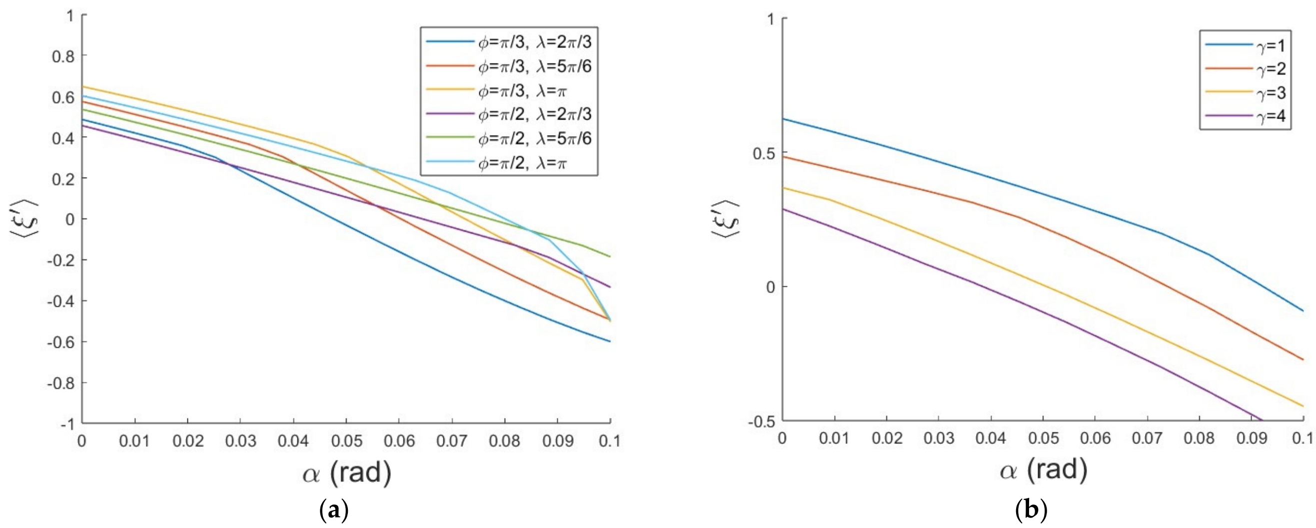

Figure 9. Non-dimensional average velocity vs. α: (**a**) μ_0 = 0.2, $\langle\mu_m\rangle/\mu_0$ = 1/5, γ = 1; (**b**) μ_0 = 0.2, $\langle\mu_m\rangle/\mu_0$ = 1/5, $\lambda = \pi$, $\phi = \pi/2$.

3.2. Experimental Results

An experimental investigation has been carried out on the technical feasibility of transporting objects on an inclined plane oscillating in its longitudinal direction, applying an additional asymmetry achieved through dynamic dry friction manipulations. The object's motion was achieved by tuning the control parameters ϕ and λ, where the dynamic effective dry friction was reduced between the object and the manipulated surface, and a frictional asymmetry was achieved. The amplitude of the sinusoidal harmonic oscillations was A = 1.04 mm, and the angular frequency was ω = 62.83 rad/s. The kinetic friction coefficient between the manipulation surface and the upward-moving object was approximately μ_0 = 0.24, and the ratio was $\langle\mu_m\rangle/\mu_0$ = 1/4. The average velocity sharply increased from ϕ = 0 and reached the maximum between $\phi = \pi/3$ and $\phi = \pi/2$ at $\lambda = \pi$, and then dramatically started to decrease until it reached $\phi = 2\pi/3$ at α = 0.035 rad as shown in Figure 10a. At a higher inclination angle α = 0.1 rad, the average velocity was notably decreased at $\phi = \pi/2$ and $\lambda = \pi$ due to the gravitational potential energy exerted on the moving object. Similarly, the average velocity was reduced at lower λ as a function of phase shift and reached a minimum at $\lambda = 2\pi/3$, as demonstrated in Figure 10b. These experimental findings verified the modeling results, which revealed that the phase shift ϕ had shown its effectiveness in controlling and changing the direction of the moving object at different inclination angles.

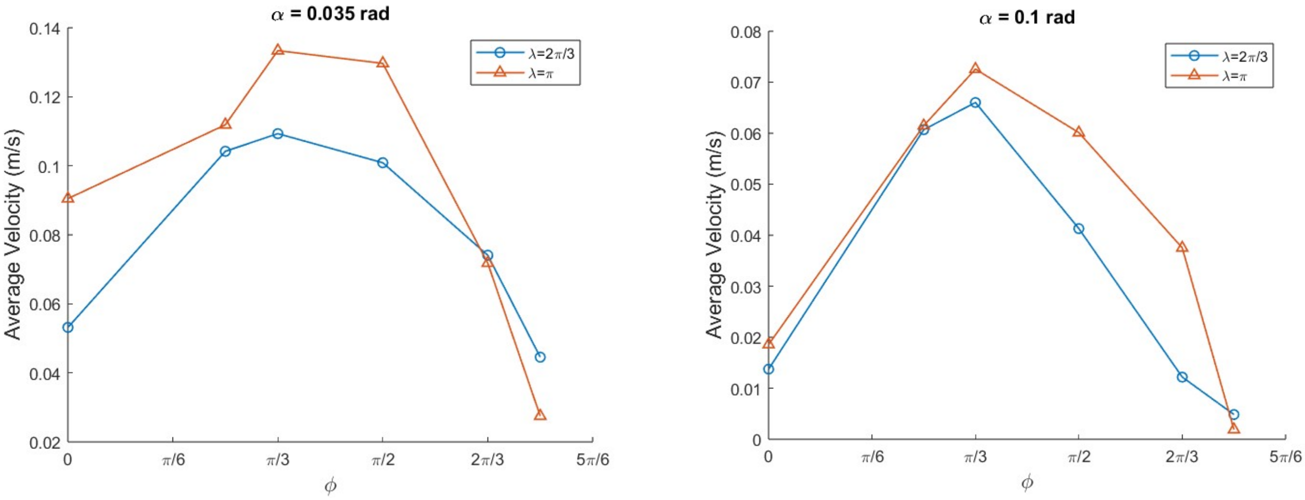

(**a**) (**b**)

Figure 10. Average transportation velocity vs. the phase shift ϕ: (**a**) α = 0.035 rad, A = 1.04 mm, ω = 62.83 rad/s; (**b**) α = 0.1 rad, A = 1.04 mm, ω = 62.83 rad/s, μ_0 = 0.24 and $\langle \mu_m \rangle / \mu_0 = 1/4$.

The experimental investigation has proven the technical feasibility of the theoretical findings that the directional motion of the moving object can be controlled by changing λ and the phase shift ϕ. Figure 11a represents the variation of the average velocity depending on λ. The average velocity was dramatically increased as λ increased between $\pi/6$ and $\pi/2$ and reached its maximum at $\phi = \pi/4$. However, as the inclination angle increased to 0.1 rad, the average velocity significantly decreased due to the gravitational potential energy, as demonstrated in Figure 11b. Similarly, the average velocity was notably increased as λ increased between $\pi/6$ and $\pi/2$. The average velocity reached the maximum at $\phi = \pi/4$ and the minimum at $\phi = \pi/2$. λ has revealed strong effectiveness in changing the velocity of the moving object at different inclination angles.

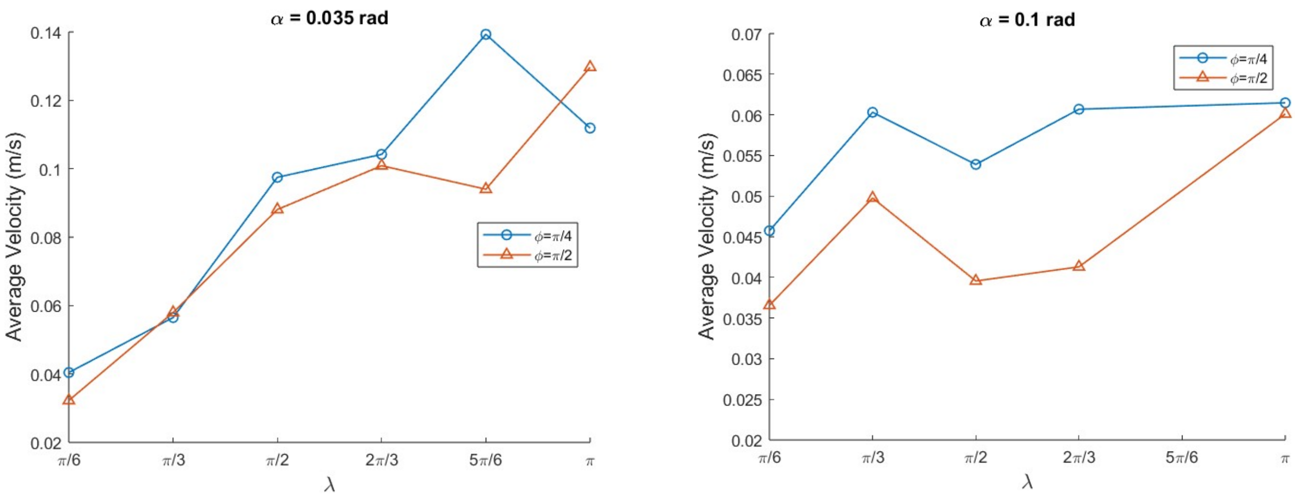

(**a**) (**b**)

Figure 11. Average transportation velocity vs. λ: (**a**) α = 0.035 rad, A = 1.04 mm, ω = 62.83 rad/s; (**b**) α = 0.1 rad, A = 1.04 mm, ω = 62.83 rad/s, μ_0 = 0.24 and $\langle \mu_m \rangle / \mu_0 = 1/4$.

Different experiments have been performed at various inclination angles α rad, as shown in Figure 12. The experiments have presented the influence of the inclined angle while the object was moving upwards. The average velocity steadily decreased as the inclined angle increased from α = 0 rad to α = 0.1 rad. The average velocity reached a maximum value at $\phi = \pi/3$ and $\lambda = \pi$, where A = 1.04 mm, ω = 62.83 rad/s, μ_0 = 0.24 and $\langle \mu_m \rangle / \mu_0 = 1/4$.

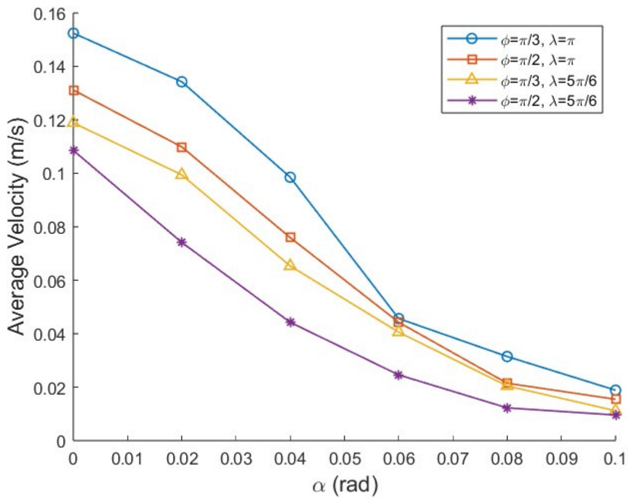

Figure 12. Average transportation velocity vs. α at A = 1.04 mm, ω = 62.83 rad/s, μ_0 = 0.24 and $\langle \mu_m \rangle / \mu_0 = 1/4$.

4. Conclusions

A mathematical model was developed to investigate the transportation of objects upward on an inclined plane that harmonically oscillates in its longitudinal direction by applying an additional asymmetry achieved through dry friction dynamic manipulations.

The modeling results have demonstrated that the asymmetry of frictional conditions that is achieved through dry friction dynamic manipulations results in a net frictional force that outweighs the gravitational force. Therefore, the object can be transported upwards. The object's velocity and direction can be changed by dynamically manipulating the dry friction coefficient to achieve the required frictional asymmetry. Also, the findings have identified the control parameters that define the moving object's directional motion. The phase shift ϕ has proven its effectiveness in controlling and changing the direction of the moving object at different inclination angles, where the average velocity was significantly increased at α = 0.035 rad between ϕ = 0 and $\phi = \pi/2$ and reached its maximum at $\lambda = \pi$. However, λ, which corresponds to the part of the period in which the friction coefficient is dynamically decreased, is a crucial parameter in changing the velocity of the object, as the average velocity was gradually increased and reached a maximum between $\lambda = \pi$ and $\lambda = 2\pi/3$ at $\phi = \pi/4$. Moreover, the results have demonstrated that the ratio of the modified effective dry friction coefficient $\langle \mu_m \rangle$ to the nominal dry friction coefficient μ_0 has a significant effect on the transportation velocity of the object. At inclination angle α = 0.035 rad, the average velocity was significantly decreased as this ratio increased, where the average velocity of the moving object reached the maximum at μ_0 = 0.15.

Experimental investigations have been carried out to prove the technical feasibility of the proposed method. The experiment has verified that periodic dynamic dry friction manipulations create an additional asymmetry that results in a net frictional force that outweighs the gravitational force acting on an object placed on an inclined plane. Therefore, the object can be transported upwards to the inclined plane. The experimental findings have shown that the control parameters ϕ and λ have a significant influence in controlling and changing the directional motion of the moving object. In agreement with the theoretical findings, the experiments demonstrated that the phase shift ϕ is very effective in controlling and changing the direction of the moving object at different inclination angles, and λ has revealed a significant influence in changing the velocity of the object being transported at different inclination angles. The experimental findings qualitatively verified the modeling by demonstrating a similar response of motion parameters to the control parameters as it was obtained in the modeling results.

The proposed transportation method is beneficial for various modern industries engaged in transportation and manipulation tasks with objects spanning a broad range of sizes, including those operating at small scales for applications in lab-on-a-chip technology, micro-assembly lines, micro-feeder systems and other delicate component manipulation systems. The method's straightforward technical implementation makes it a cost-effective alternative to more intricate devices like microgrippers. The presented research advances the classical theories of vibrational transportation on inclined surfaces. Future research will focus on further developing and optimizing the proposed transportation method to handle large quantities of small-scale materials, microelectronics components and similar micro-scale particles.

Author Contributions: Conceptualization, R.E.B., A.F. and S.K.; methodology, R.E.B., A.F. and S.K.; software, R.E.B., K.L. and S.K.; validation, R.E.B.; formal analysis, R.E.B., K.L., V.L. and S.K.; investigation, R.E.B.; resources, R.E.B. and S.K.; data curation, R.E.B.; writing—original draft preparation, R.E.B.; writing—review and editing, R.E.B., K.L., V.L. and S.K.; visualization, R.E.B.; supervision, S.K. All authors have read and agreed to the published version of the manuscript.

Funding: This research received no external funding.

Institutional Review Board Statement: Not applicable.

Informed Consent Statement: Not applicable.

Data Availability Statement: The data presented in this study are available on request from the corresponding author. The data are not publicly available due to the ongoing research.

Conflicts of Interest: The authors declare no conflicts of interest.

References

1. Takosoglu, J.; Galkiewics, U.; Galkiewics, J. A Design of a 2 DoF Planar Parallel Manipulator with an Electro-Pneumatic Servo-Drive–Part 2. *Energies* **2023**, *16*, 2970. [CrossRef]
2. Bialek, M.; Jedryczka, C. Design and Optimization of a Magnetic Field Exciter for Controlling Magnetorheological Fluid in a Hybrid Soft-Rigid Jaw Gripper. *Energies* **2023**, *16*, 2299. [CrossRef]
3. Ruggiero, F.; Lippiello, V.; Siciliano, B. Nonprehensile dynamic manipulation: A survey. *IEEE Robot. Autom. Lett.* **2018**, *3*, 1711–1718. [CrossRef]
4. Reznik, D.; Canny, J.; Goldberg, K. Analysis of part motion on a longitudinally vibrating plate. In Proceedings of the 1997 IEEE/RSJ International Conference on Intelligent Robot and Systems, Grenoble, France, 11 September 1997; IEEE: Piscataway, NJ, USA, 1997; pp. 421–427. [CrossRef]
5. Viswarupachari, C.; DasGupta, A.; Pratik Khastgir, S. Vibration induced directed transport of particles. *J. Vib. Acoust.* **2012**, *134*, 051005. [CrossRef]
6. Mayyas, M. Modeling and analysis of vibratory feeder system based on robust stick–slip motion. *J. Vibrat. Control.* **2021**, *28*, 2301–2309. [CrossRef]
7. Mayyas, M. Parallel Manipulation Based on Stick-Slip Motion of Vibrating Platform. *Robotics* **2020**, *9*, 86. [CrossRef]
8. Hunnekens, B.G.B.; Fey, R.H.B.; Shukla, A. Vibrational self-alignment of a rigid object exploiting friction. *Nonlinear Dyn.* **2010**, *65*, 109–129. [CrossRef]
9. Higashimori, M.; Yamaguchi, K.; Shibata, A. Omnidirectional Nonprehensile Manipulation Using Only One Actuator. *Robotics* **2018**, *7*, 34. [CrossRef]
10. Sakashita, R.; Higashimori, M. 1-actuator 3-DoF parts feeding using hybrid joint mechanism with twisted axis layout. In Proceedings of the 2017 IEEE International Conference on Robotics and Automation (ICRA), Singapore, 29 May–3 June 2017; IEEE: Piscataway, NJ, USA, 2017; pp. 2335–2342. [CrossRef]
11. Yamaguchi, K.; Higashimori, M. 1-Actuator 3-DoF Manipulation Using a Virtual Turntable Based on Differential Friction Surface. In Proceedings of the 2018 IEEE International Conference on Robotics and Automation, Brisbane, Australia, 21–25 May 2018; IEEE: Piscataway, NJ, USA, 2018; pp. 3573–3580. [CrossRef]
12. Chen, H.; Jiang, S.; Liu, R.; Zhang, W. Particle Directional Conveyance under Longitudinal Vibration by considering the Trough Surface Texture: Numerical Simulation Based on the Discrete Element Method. *Shock. Vibrat.* **2018**, *2018*, 8260462. [CrossRef]

13. Vrublevskyi, I. Vibratory conveying by harmonic longitudinal and polyharmonic normal vibrations of inclined conveying track. *J. Vib. Acoust.* **2022**, *144*, 011004. [CrossRef]
14. Gursky, V.; Krot, P.; Korendiy, V.; Zimroz, R. Dynamic Analysis of an Enhanced Multi-Frequency Inertial Exciter for Industrial Vibrating Machines. *Machines* **2022**, *10*, 130. [CrossRef]
15. Schiller, S.; Perchtold, D.; Steiner, W. Nonlinear and chaotic dynamics of a vibratory conveying system. *Nonlinear Dyn.* **2023**, *111*, 9799–9814. [CrossRef]
16. Klemiato, M.; Czubak, P. Control of the transport direction and velocity of the two-way reversible vibratory conveyor. *Arch. Appl. Mech.* **2019**, *89*, 1359–1373. [CrossRef]
17. Baksys, B.; Baskutiene, J. The directional motion of the compliant body under vibratory excitation. *Int. J. Non Linear Mech.* **2012**, *47*, 3. [CrossRef]
18. Baksys, B.; Puodziuniene, N. Modeling of vibrational non-impact motion of mobile-based body. *Int. J. Non Linear Mech.* **2012**, *40*, 6. [CrossRef]
19. Chen, Z.; Liu, X.; Kojima, M.; Huang, Q.; Arai, T. Advances in Micromanipulation Actuated by Vibration-Induced Acoustic Waves and Streaming Flow. *Appl. Sci.* **2020**, *10*, 1260. [CrossRef]
20. Kumar, A.; DasGupta, A. Generation of circumferential harmonic travelling waves on thin circular plates. *J. Sound. Vib.* **2020**, *478*, 115343. [CrossRef]
21. Kilikevičius, S.; Liutkauskiene, K.; Fedaravičius, A. Nonprehensile Manipulation of Parts on a Horizontal Circularly Oscillating Platform with Dynamic Dry Friction Control. *Sensors* **2021**, *21*, 5581. [CrossRef]
22. Kilikevičius, S.; Liutkauskienė, K.; Uldinskas, E.; El Banna, R.; Fedaravičius, A. Omnidirectional Manipulation of Microparticles on a Platform Subjected to Circular Motion Applying Dynamic Dry Friction Control. *Micromachines* **2022**, *13*, 5. [CrossRef]
23. Benad, J.; Benad, J.; Nakano, K.; Nakano, K.; Popov, V.; Popov, V.; Popov, M.; Popov, M. Active control of friction by transverse oscillations. *Friction* **2019**, *7*, 74–85. [CrossRef]
24. Popov, V.L.; Starcevic, J.; Filippov, A.E. Influence of ultrasonic in-plane oscillations on static and sliding friction and intrinsic length scale of dry friction processes. *Tribol. Lett.* **2010**, *39*, 25–30. [CrossRef]
25. Menga, N.; Bottiglione, F.; Carbone, G. Dynamically induced friction reduction in micro-structured interfaces. *Sci. Rep.* **2021**, *11*, 8094. [CrossRef] [PubMed]
26. Storck, H.; Littmann, W.; Wallaschek, J.; Mracek, M. The effect of friction reduction in presence of ultrasonic vibrations and its relevance to travelling wave ultrasonic motors. *Ultrasonics* **2002**, *40*, 379–383. [CrossRef] [PubMed]
27. Littmann, W.; Storck, H.; Wallaschek, J. Sliding friction in the presence of ultrasonic oscillations: Superposition of longitudinal oscillations. *Arch. Appl. Mech.* **2001**, *71*, 549–554. [CrossRef]